JOURNAL OF SOLID STATE CHEMISTRY 114, 399–405 (1995)

Synthesis and Structure of $K_{2x}Ba_{2-x}Sb_4O_9(PO_4)_2$ ($0 < x < 0.4$)

C. Pagnoux, A. Mar, A. Verbaere, and Y. Piffard[1]

Laboratoire de Chimie des Solides, UMR 110, CNRS, Université de Nantes, 2 rue de la Houssinière, 44072 Nantes Cedex 03, France

Received November 23, 1993; accepted May 12, 1994

The solid solution $K_{2x}Ba_{2-x}Sb_4O_9(PO_4)_2$ ($0 < x < 0.4$) has been prepared, and the structures of the end members $K_{0.8}Ba_{1.6}Sb_4O_9(PO_4)_2$ and $Ba_2Sb_4O_9(PO_4)_2$ have been determined from single-crystal and powder diffraction data, respectively. The compounds crystallize in space group *Pnma* of the orthorhombic system with $Z = 4$ in cells of dimensions $a = 20.998(3)$, $b = 7.168(1)$, and $c = 9.569(2)$ Å for $K_{0.8}Ba_{1.6}Sb_4O_9(PO_4)_2$ and $a = 20.9237(6)$, $b = 7.1836(2)$, and $c = 9.5189(3)$ Å for $Ba_2Sb_4O_9(PO_4)_2$. Their structure consists of a three-dimensional arrangement of corner-sharing SbO_6 octahedra and PO_4 tetrahedra. In $K_{0.8}Ba_{1.6}Sb_4O_9(PO_4)_2$, the K and Ba atoms are partially ordered among four possible sites, while in $Ba_2Sb_4O_9(PO_4)_2$, the Ba atoms occupy only two of these sites. Arguments for the distribution of the K and Ba atoms in $K_{0.8}Ba_{1.6}Sb_4O_9(PO_4)_2$ are presented.

INTRODUCTION

As part of a search for materials likely to exhibit fast alkali-ion transport or facile ion-exchange properties, we have been investigating the systems A_2O–Sb_2O_5–P_2O_5 (A = alkali metal), whose structures typically consist of a highly covalent framework of SbO_6 octahedra and PO_4 tetrahedra. For example, the compounds KSb_2PO_8 (1) and $K_5Sb_5P_2O_{20}$ (2) possess three-dimensional frameworks forming wide tunnels in which the K cations are situated, $K_3Sb_3P_2O_{14}$ (3) and $KSbP_2O_8$ (4) possess covalent layers between which lie easily exchangeable K cations, and K_2SbPO_6 (5) forms one-dimensional chains separated by K cations.

We have recently extended our studies to include an alkaline earth metal: K_2O–BaO–Sb_2O_5–P_2O_5. Because the size of a Ba^{2+} cation (1.35 Å) is close to that of a K^+ cation (1.38 Å) (6), one would expect it to retain structural features similar to those found in the K–Sb–P–O compounds, chiefly the open covalent frameworks so necessary for ionic mobility. However, the higher charge of the Ba^{2+} cation may lead to its preferential occupation of certain cation sites, being more tightly bound and less likely to undergo exchange.

[1] To whom correspondence should be addressed.

We report here the preparation and crystal structure of $K_{0.8}Ba_{1.6}Sb_4O_9(PO_4)_2$, and the confirmation of the location of Ba atoms from a powder refinement of $Ba_2Sb_4O_9(PO_4)_2$.

EXPERIMENTAL

Synthesis. The different members of the solid solution $K_{2x}Ba_{2-x}Sb_4O_9(PO_4)_2$ ($0 < x < 0.4$) were prepared from mixtures of the reactants KNO_3, $Ba(NO_3)_2$, $Sb_2O_5 \cdot nH_2O$, and $NH_4H_2PO_4$, in stoichiometric proportions. The mixtures were heated in platinum crucibles at temperatures between 673 and 873 K for 3 hr to decompose the nitrates, and then heated at 1253 K for 10 hr in air. In the solid solution regime $0 < x < 0.4$, only single-phase material was detected by X-ray powder diffraction. Above $x = 0.4$, a second phase $K_3Sb_3P_2O_{14}$ (3) forms as an impurity, lending support to the assertion that $K_{0.8}Ba_{1.6}Sb_4O_9(PO_4)_2$ represents the upper compositional limit of the solid solution.

Single crystals of $K_{0.8}Ba_{1.6}Sb_4O_9(PO_4)_2$ were obtained by taking a mixture of KNO_3, $Ba(NO_3)_2$, $Sb_2O_5 \cdot nH_2O$, and $NH_4H_2PO_4$ in a 1 : 1 : 1 : 2 ratio and subjecting it to a heat treatment similar to that described above, except that the temperature was raised to 1373 K in the second step. The crystals are colorless needles that grow along the [010] direction. An energy-dispersive microprobe analysis of these crystals with a scanning electron microscope revealed the presence of the elements K, Ba, Sb, and P in a 0.8 : 1.6 : 4.0 : 2.0 ratio, the compound KSb_2PO_8 (1) having served as a reference standard. We accept this analysis to be representative of the composition of these crystals, coupled with the observation that single-phase material can only be prepared for a loading composition $K_{2x}Ba_{2-x}Sb_4O_9(PO_4)_2$ with $x < 0.4$.

The other members of the series, in particular the lower limit $Ba_2Sb_4O_9(PO_4)_2$, could only be prepared in the form of powders.

Structure determination of $K_{0.8}Ba_{1.6}Sb_4O_9(PO_4)_2$. Initial photographic work revealed orthorhombic symmetry and provided preliminary cell parameters. Single-crystal intensity data were collected at room temperature on an Enraf–Nonius CAD4 diffractometer under the conditions

0022-4596/95 $6.00

given in Table 1. The powder pattern was recorded on an INEL multidetector system, with the use of a 0.2-mm capillary and Cu$K\alpha_1$ radiation (λ = 1.54059 Å; Si standard). Table 2 compares observed interplanar distances and the values calculated from the single-crystal structure with the use of the program LAZY-PULVERIX (7).

Data reduction, structure solution, and refinements were carried out using programs in the MOLEN package (8). Analysis of the intensity data, collected in the unique octant $+h$, $+k$, $+l$, revealed the systematic absences ($0kl$, $k + l = 2n + 1$; $hk0$, $h = 2n + 1$), which are consistent with the space groups *Pnma* and $Pn2_1a$. The structure was solved and refined satisfactorily in the centrosymmetric space group *Pnma*. Conventional atomic scattering factors were used (9). A Gaussian-type absorption correction was applied to the intensity data (10). The positions of the Ba and Sb atoms were located from the Patterson map, and the remaining atoms were found in subsequent difference Fourier syntheses. The structure was then refined by least-squares methods.

TABLE 1
Experimental Details of the Crystallographic Study of $K_{0.8}Ba_{1.6}Sb_4O_9(PO_4)_2$ and $Ba_2Sb_4O_9(PO_4)_2$

Formula	$K_{0.8}Ba_{1.6}Sb_4O_9(PO_4)_2$	$Ba_2Sb_4O_9(PO_4)_2$
Formula mass (amu)	1071.94	1095.59
Sample	Single crystal of dimensions 0.012 × 0.20 × 0.20 mm	Powder sieved at 20 μm
a (Å)	20.998(3)	20.9237(6)
b (Å)	7.168(1)	7.1836(2)
c (Å)	9.569(2)	9.5189(3)
V (Å^3)	1440.3(7)	1430.76(9)
Space group	*Pnma*	*Pnma*
Z	4	4
ρ_c (g cm^{-3})	4.94	5.09
μ(Mo$K\alpha$) (cm^{-1})	121.0	
F(000)	1899	1928
Diffractometer used	CAD4	INEL multidetector
Radiation	Mo$K\alpha$, λ = 0.71069 Å	Cu$K\alpha_1$, λ = 1.54059 Å
Scan	$\theta - 2\theta$	simultaneous detection
Scan angle $\Delta\omega$ (deg.)	1.2 + 0.35 tan θ	
2θ limits (°)	4.0–60.0	9.5–110.0
Refinement method	Single crystal refinement	Rietveld powder refinement
No. of data collected	3608 reflections, of which 1453 have $I > 3\sigma(I)$	3346 data points; 991 reflections with $I > 1\sigma(I)$
Transmission factors	0.22–0.83	
No. of variables	94 (including anisotropic temperature factors)	26 (including 9 atomic parameters)
Agreement factors	R = 0.032 R_w = 0.037	R_I = 0.115 R_p = 0.046 R_{wp} = 0.062 R_{exp} = 0.030

In the course of intermediate refinements and difference Fourier syntheses, it became evident that, of the four possible sites found for the Ba and K atoms (Table 3) some would have to be partially occupied or partially disordered to account for the presumed chemical formula as well as to arrive at reasonable values for the thermal parameters. Thus, the Ba and K atoms were distributed such that: (i) the first site contained only Ba atoms at full occupancy; (ii) the second site contained Ba atoms at 40% occupancy; (iii) the third site, located very close to the second site (0.4 Å away along the a direction), was partially occupied as well as disordered (20% Ba, 30% K); and (iv) the fourth site contained K atoms at 50% occupancy. Refinements on models with other distributions of Ba and K atoms consistent with the composition $K_{0.8}Ba_{1.6}Sb_4O_9(PO_4)_2$ lead to generally unreasonable values for the thermal parameters. Moreover, the difference Fourier map shows that there is a discrete splitting of the close second and third sites that cannot arise from an artifact of unusually elongated thermal motion. Further support for this distribution can be found from the results of the refinement on $Ba_2Sb_4O_9(PO_4)_2$ as well as from chemical arguments (*vide infra*).

At this stage, anisotropic temperature factors were refined for the Ba(1), K(2), Sb, and P atoms. The final cycle of refinement on reflections with $I > 3\sigma(I)$ included an extinction parameter (g = 5.6(3) × 10^{-8}) and converged to values of R = 0.032 and R_w = 0.037. The final difference electron density map shows no residuals greater than 1.3 e Å^{-3}. The final positional and thermal parameters are given in Tables 3a and 3b. (A table of structure factors is available from the authors upon request.)

Rietveld refinement of $Ba_2Sb_4O_9(PO_4)_2$. In order to find further evidence for the proposed distribution of Ba and K atoms in $K_{0.8}Ba_{1.6}Sb_4O_9(PO_4)_2$, it was of interest to determine the structure of $Ba_2Sb_4O_9(PO_4)_2$. X-ray powder diffraction data on a sample contained in a glass Lindemann capillary of 0.2 mm diameter were accumulated over 4 hr on an INEL multidetector system with the use of Cu$K\alpha_1$ radiation. Data reduction and Rietveld refinements were carried out with the use of programs in the GSAS package (11). Further details of the data collection and structure refinement are given in Table 1. The peak profiles were fitted by a Gaussian-type function, modified for peak asymmetry and involving four parameters (12). In addition, eight Fourier coefficients for the background, four parameters for the peak positions (cell constants and origin), and one scale factor were used.

The initial atomic positions of $Ba_2Sb_4O_9(PO_4)_2$ were taken from those determined in the single-crystal X-ray structure of $K_{0.8}Ba_{1.6}Sb_4O_9(PO_4)_2$, in space group *Pnma*. Two sites were chosen in which the Ba atoms were initially placed: Ba(1), identical to that found in $K_{0.8}Ba_{1.6}Sb_4O_9(PO_4)_2$, and Ba(2), at a position intermedi-

TABLE 2
X-ray Powder Diffraction Pattern of $K_{0.8}Ba_{1.6}Sb_4O_9(PO_4)_2$

hkl	d_{obs} (Å)	d_{calc} (Å)	I/I_0	*hkl*	d_{obs} (Å)	d_{calc} (Å)	I/I_0
101	8.695	8.707	85	611	2.988	2.988	27
201	7.057	7.072	48	420		2.958	5
301	5.647	5.649	11	303	2.904	2.902	100
111	5.523	5.534	16	512	2.888	2.888	12
400		5.250	3	701		2.863	3
211	5.030	5.034	38	122	2.843	2.842	65
002	4.778	4.784	7	421	2.829	2.828	44
311	4.432	4.437	9	213	2.808	2.808	13
202	4.352	4.354	17	222	2.767	2.767	21
410	4.232	4.235	10	313	2.691	2.690	8
302		3.950	4	711	2.658	2.658	14
112	3.903	3.910	9	521	2.623	2.632	8
501	3.841	3.846	31	801	2.532	2.531	22
212		3.720	5	422	2.517	2.517	12
402	3.535	3.536	19	620	2.505	2.504	10
600	3.499	3.500	34	712	2.394	2.395	4
312	3.454	3.460	9	231		2.261	3
121	3.313	3.314	70	721	2.238	2.237	14
601		3.287	5	622		2.218	4
221	3.197	3.197	71	331		2.199	3
412	3.171	3.171	11	314	2.159	2.159	7
502	3.156	3.156	32	713	2.089	2.090	11
610	3.149	3.145	33	504	2.079	2.079	8
321		3.024	5	722	2.074	2.073	12

ate between those of the Ba(2) and Ba(3)/K(1) sites in $K_{0.8}Ba_{1.6}Sb_4O_9(PO_4)_2$. An overall isotropic thermal parameter was applied to each type of atom, and at later stages of the refinement, the absorption coefficient was adjusted in order to obtain positive B values for all atoms. In all refinements, the positions of the P and O atoms were kept fixed because: (i) they are highly correlated with the thermal and profile parameters; (ii) the intensities are largely dominated by the heavier Ba and Sb atoms; and (iii) there are insufficient data to justify the refinement of many more atomic parameters and expect to arrive at meaningful results. Indeed, attempts to refine the P and O positions invariably result in shifts, which, though slight, lead to a few bond distances and angles being chemically unsatisfactory.

At this stage, the Ba(1) atom experienced little change in its position, while the Ba(2) atom shifted significantly such that it was now much closer to the corresponding Ba(2) than the Ba(3)/K(1) site of $K_{0.8}Ba_{1.6}Sb_4O_9(PO_4)_2$. When the occupancies of the Ba(1) and Ba(2) sites are refined, they converge to values of 103(1)% and 104(1)%, respectively, with no improvement in R_{wp} (0.062). Finally, when one attempts to introduce models in which there is partial occupation of the Ba(2) with either the Ba(3)/K(1) or the K(2) site, their occupancies converge to 0(2)% and 2(1)%, respectively. These results clearly demonstrate that, in $Ba_2Sb_4O_9(PO_4)_2$, the Ba atoms fully occupy the Ba(1) and Ba(2) sites and do not occupy the Ba(3)/K(1) and K(2) sites of $K_{0.8}Ba_{1.6}Sb_4O_9(PO_4)_2$. The final difference Fourier map is featureless, with extrema of +5.7 and −4.5 e Å^{-3}, further confirming the validity of this model. The final positional parameters of the Ba and Sb atoms are given in Table 3a, and the final Rietveld profile fit is shown in Fig. 1.

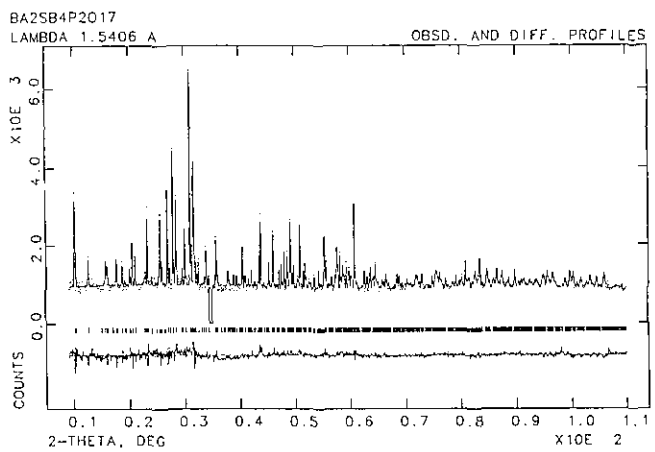

FIG. 1. Final Rietveld profile fit of $Ba_2Sb_4O_9(PO_4)_2$: observed data (···); calculated profile (—). The reflection positions are indicated by vertical markers. The difference plot (observed minus calculated) is shown by the lower trace on the same scale. The excluded region between 34.5° and 35.0° contains a small impurity peak.

TABLE 3a

Positional and Thermal Parameters for $K_{0.8}Ba_{1.6}Sb_4O_9(PO_4)_2$ and $Ba_2Sb_4O_9(PO_4)_2$

Atom	Wyckoff position	Occupancy	x	y	z	B_{iso}/B_{eq}[a] (Å^2)
			$K_{0.8}Ba_{1.6}Sb_4O_9(PO_4)_2$			
Ba(1)	4*c*	1	0.47173(4)	0.25	0.15531(9)	1.26(1)[a]
Ba(2)	4*c*	0.4	0.17596(9)	0.25	0.1895(2)	0.71(3)
Ba(3)/K(1)	4*c*	0.2/0.3	0.1570(2)	0.25	0.1897(4)	1.52(5)
K(2)	4*c*	0.5	0.2903(3)	0.25	0.9963(7)	1.8(1)[a]
Sb(1)	8*d*	1	0.34175(2)	0.9990(1)	0.32994(5)	0.353(6)[a]
Sb(2)	4*a*	1	0	0	0	0.334(9)[a]
Sb(3)	4*c*	1	0.27583(4)	0.25	0.62975(9)	0.41(1)[a]
P(1)	4*c*	1	0.1289(2)	0.25	0.5493(3)	0.50(5)[a]
P(2)	4*c*	1	0.4268(2)	0.25	0.7475(3)	0.49(5)[a]
O(1)	4*c*	1	0.0312(4)	0.25	0.0437(9)	0.6(1)
O(2)	4*c*	1	0.1991(5)	0.25	0.504(1)	0.9(1)
O(3)	4*c*	1	0.0881(5)	0.25	0.421(1)	1.0(1)
O(4)	8*d*	1	0.4311(3)	0.047(1)	0.3728(7)	0.77(9)
O(5)	8*d*	1	0.2424(3)	0.0484(9)	0.7482(7)	0.62(9)
O(6)	8*d*	1	0.1185(3)	0.071(1)	0.6393(7)	1.0(1)
O(7)	4*c*	1	0.3533(5)	0.25	0.755(1)	0.9(1)
O(8)	4*c*	1	0.3365(5)	0.25	0.251(1)	0.8(1)
O(9)	4*c*	1	0.1519(4)	0.25	0.9014(9)	0.3(1)
O(10)	8*d*	1	0.3111(3)	0.0519(9)	0.5160(6)	0.68(9)
O(11)	8*d*	1	0.4466(3)	0.075(1)	0.6653(7)	1.0(1)
O(12)	4*c*	1	0.4528(5)	0.25	0.891(1)	1.4(2)
			$Ba_2Sb_4O_9(PO_4)_2$[b]			
Ba(1)	4*c*	1	0.4716(3)	0.25	0.1506(6)	1.0
Ba(2)	4*c*	1	0.1746(3)	0.25	0.1911(7)	1.0
Sb(1)	8*d*	1	0.3417(2)	0.9996(7)	0.3304(4)	0.5
Sb(2)	4*a*	1	0	0	0	0.5
Sb(3)	4*c*	1	0.2778(3)	0.25	0.6349(7)	0.5

[a] $B_{eq} = \frac{4}{3} \Sigma_i \Sigma_j \beta_{ij} \mathbf{a}_i \cdot \mathbf{a}_j$.

[b] The P and O atoms were fixed at positions occurring in $K_{0.8}Ba_{1.6}Sb_4O_9(PO_4)_2$, with temperature factors of 0.5 and 0.8, respectively. See text for details.

TABLE 3b

Anisotropic Thermal Parameters[a] (Å^2) in $K_{0.8}Ba_{1.6}Sb_4O_9(PO_4)_2$

Atom	U_{11}	U_{22}	U_{33}	U_{12}	U_{13}	U_{23}
Ba(1)	0.0139(3)	0.0232(4)	0.0108(3)	0	0.0034(3)	0
K(2)	0.022(3)	0.040(4)	0.007(2)	0	−0.009(2)	0
Sb(1)	0.0048(2)	0.0036(2)	0.0051(2)	−0.0007(2)	−0.0006(2)	−0.0003(2)
Sb(2)	0.0041(2)	0.0033(3)	0.0053(2)	0.0002(3)	0.0004(2)	−0.0004(3)
Sb(3)	0.0049(3)	0.0043(3)	0.0063(3)	0	0.0019(3)	0
P(1)	0.004(1)	0.008(1)	0.006(1)	0	−0.002(1)	0
P(2)	0.006(1)	0.008(1)	0.005(1)	0	−0.000(1)	0

[a] The form of the anisotropic thermal parameter is $\exp[-2\pi^2(h^2a^{*2}U_{11} + k^2b^{*2}U_{22} + l^2c^{*2}U_{33} + 2hka^*b^*U_{12} + 2hla^*c^*U_{13} + 2klb^*c^*U_{23})]$.

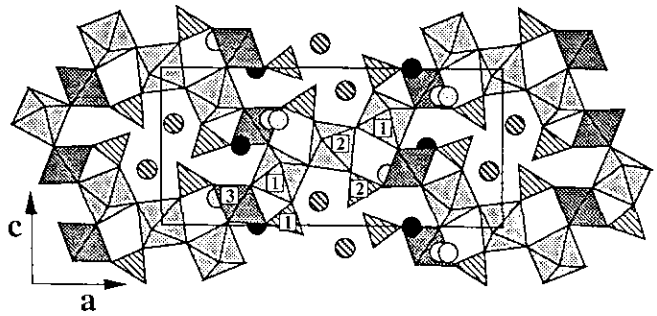

FIG. 2. View of $K_{0.8}Ba_{1.6}Sb_4O_9(PO_4)_2$ along the [010] direction. The light-shaded polyhedra represent $Sb(1)O_6$–$Sb(2)O_6$–$Sb(1)O_6$ octahedra, the dark-shaded polyhedra represent $Sb(3)O_6$ octahedra, and the hatched polyhedra represent PO_4 tetrahedra.

RESULTS AND DISCUSSION

Description of the structure. Views of the structure of $K_{0.8}Ba_{1.6}Sb_4O_9(PO_4)_2$ along the *b* and *c* axes are given in Figs. 2 and 3, respectively. The covalent framework is composed of a three-dimensional arrangement of SbO_6 octahedra and PO_4 tetrahedra linked only by their corners. The octahedral network can be regarded as containing ribbons of $Sb(1)O_6$ and $Sb(2)O_6$ octahedra. Each ribbon contains three corner-sharing octahedral chains $Sb(1)O_6$–$Sb(2)O_6$–$Sb(1)O_6$ extending infinitely along the *b* direction, thus forming a fragment, albeit a distorted one, of the ReO_3 structure. The octahedra, lying at $y = 0$ and $\frac{1}{2}$, are tilted to form staggered chains with Sb(1)–O–Sb(1) angles of 133.9(5)°–137.3(4)° and Sb(2)–O–Sb(2) angles of 133.1(5)°. These $Sb(1)O_6$–$Sb(2)O_6$–$Sb(1)O_6$ ribbons are then connected by $Sb(3)O_6$ octahedra, lying at $y = \frac{1}{4}$ and $\frac{3}{4}$, which link with corners of the $Sb(1)O_6$ octahedra. The PO_4 tetrahedra are attached to the octahedral network: the $P(1)O_4$ tetrahedra share two vertices with $Sb(1)O_6$ and one vertex with $Sb(3)O_6$, and the $P(2)O_4$ tetrahedra share two vertices with $Sb(2)O_6$ and one vertex with $Sb(3)O_6$. In both types of PO_4 tetrahedra, one vertex remains unattached and points to large cavities in the structure, in which the Ba and K atoms are located. A closely related structure is that of $Tl_3NaNb_4O_9(PO_4)_2$ (13), in which the octahedral triple-chain ribbon is bent rather than straight; the different connectivity of these ribbons alters the shape of the large cavities slightly.

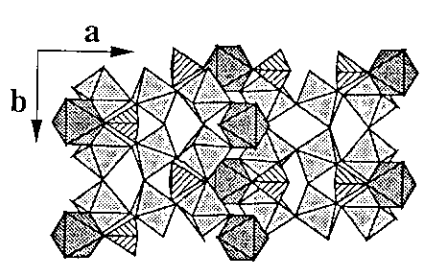

FIG. 3. View of $K_{0.8}Ba_{1.6}Sb_4O_9(PO_4)_2$ along the [001] direction.

Table 4 lists some distances and angles around the various coordination polyhedra. These values are unexceptional and correspond well with those found in previously known phosphatoantimonates (1–5). The Sb–O distances range from 1.914(3) to 2.068(7) Å in $Sb(1)O_6$, forming a slightly distorted octahedron, while they range from 1.921(6) to 2.014(7) Å in $Sb(2)O_6$ and from 1.936(7) to 2.01(1) Å in $Sb(3)O_6$, forming fairly regular octahedra. As is usually observed, the P–O distances associated with the unshared oxygen atoms of the PO_4 tetrahedra are shorter than the other three (1.49(1) vs 1.54(1)–1.561(8) Å for $P(1)O_4$; 1.48(1) vs 1.536(8)–1.55(1) Å for $P(2)O_4$).

Occupation of Ba and K sites. Of particular importance is the way in which the Ba and K atoms occupy the cation sites, four of which are possible in $K_{0.8}Ba_{1.6}Sb_4O_9(PO_4)_2$. In the corresponding $Ba_2Sb_4O_9(PO_4)_2$ structure, the results of the powder refinement confirm that the Ba atoms reside entirely at the Ba(1) and Ba(2) sites. This observation strongly suggests that these are the more energetically favorable sites for Ba atoms, and they should also be likewise preferentially occupied in $K_{0.8}Ba_{1.6}Sb_4O_9(PO_4)_2$. The higher positive charge of the Ba^{2+} cations represents a dominating electrostatic constraint and will tend to dictate their preferred placement at these sites, after which the K^+ cations must then content themselves with less favorable sites. Thus, the Ba(1) site, which is located in a large cavity formed by the phosphatoantimonate network and for which the number of short contacts to oxygen atoms is maximized, is found to be entirely occupied by Ba atoms. The Ba(2) site is the next most favorable, but it probably has a relatively soft potential, for there is another nearby minimum only 0.4 Å away that represents the Ba(3)/K(1) site, which is partially occupied by both Ba and K atoms. The combined total occupancy of the Ba(2) and Ba(3)/K(1) sites cannot, of course, exceed one, so that the remaining K atoms occupy the least favorable site, K(2). The K(2) site is only 3.032(7) Å away from the Ba(2) site, and once it begins to be occupied by K atoms, there arises a concomitant impetus for depopulating the Ba(2) site to reduce the electrostatic repulsion; thus, the nearby Ba(3)/K(1) site, at a distance of 3.359(7) Å from the K(2) site, accommodates a mixture of Ba and K atoms. It would appear, then, that the equilibrium distribution of Ba and K atoms results from an electrostatic compromise between the need to maximize cation–oxygen bonding interactions while minimizing cation–cation repulsions.

With these remarks, it may be understood why the solid

TABLE 4
Selected Interatomic Distances (Å) and Angles (°) in $K_{0.8}Ba_{1.6}Sb_4O_9(PO_4)_2$

			$Sb(1)O_6$ octahedron[a]			
Sb(1)	O(4)^{i}	O(5)^{ii}	O(6)^{ii}	O(8)^{i}	O(9)^{ii}	O(10)^{i}
O(4)^{i}	1.953(6)	3.898(9)	2.607(9)	2.73(1)	2.764(9)	2.871(9)
O(5)^{ii}	168.6(3)	1.964(6)	2.809(9)	2.705(9)	2.80(1)	2.892(9)
O(6)^{ii}	80.8(3)	88.3(3)	2.068(7)	2.704(9)	2.91(1)	3.996(9)
O(8)^{i}	88.5(4)	87.3(3)	84.4(3)	1.953(4)	3.867(5)	2.96(1)
O(9)^{ii}	91.2(3)	92.5(3)	93.6(3)	178.1(4)	1.914(3)	2.546(8)
O(10)^{i}	95.3(3)	95.8(3)	174.7(3)	99.1(3)	82.9(3)	1.932(6)
			$Sb(2)O_6$ octahedron[a]			
Sb(2)	O(1)	O(1)^{iii}	O(4)^{iv}	O(4)^{v}	O(11)^{iv}	O(11)^{v}
O(1)	1.952(4)	3.903(7)	2.797(9)	2.68(1)	2.645(9)	2.95(1)
O(1)^{iii}	180	1.952(4)	2.68(1)	2.797(9)	2.95(1)	2.645(9)
O(4)^{iv}	92.5(3)	87.5(3)	1.921(6)	3.84(1)	2.827(9)	2.738(9)
O(4)^{v}	87.5(3)	92.5(3)	180	1.921(6)	2.738(9)	2.827(9)
O(11)^{iv}	83.7(3)	96.3(3)	91.8(3)	88.2(3)	2.014(7)	4.03(1)
O(11)^{v}	96.3(3)	83.7(3)	88.2(3)	91.8(3)	180	2.014(7)
			$Sb(3)O_6$ octahedron[a]			
Sb(3)	O(2)	O(5)	O(5)^{vi}	O(7)	O(10)	O(10)^{vi}
O(2)	2.01(1)	2.89(1)	2.89(1)	4.03(1)	2.75(1)	2.75(1)
O(5)	93.4(3)	1.965(7)	2.89(1)	2.74(1)	2.650(9)	3.900(9)
O(5)^{vi}	93.4(3)	94.5(4)	1.965(7)	2.74(1)	3.900(9)	2.650(9)
O(7)	179.6(4)	86.8(3)	86.8(3)	2.02(1)	2.84(1)	2.84(1)
O(10)	88.3(3)	85.6(3)	178.3(3)	91.5(3)	1.936(7)	2.84(1)
O(10)^{vi}	88.3(3)	178.3(3)	85.6(3)	91.5(3)	94.2(4)	1.936(7)
			$P(1)O_4$ tetrahedron[a]			
P(1)	O(2)	O(3)	O(6)	O(6)^{vi}		
O(2)	1.54(1)	2.46(1)	2.49(1)	2.49(1)		
O(3)	108.6(6)	1.49(1)	2.53(1)	2.53(1)		
O(6)	106.9(3)	111.8(3)	1.561(8)	2.57(1)		
O(6)^{vi}	106.9(3)	111.8(3)	110.6(6)	1.561(8)		
			$P(2)O_4$ tetrahedron[a]			
P(2)	O(7)	O(11)	O(11)^{vi}	O(12)		
O(7)	1.55(1)	2.48(1)	2.48(1)	2.46(1)		
O(11)	107.2(4)	1.536(8)	2.50(1)	2.50(1)		
O(11)^{vi}	107.2(4)	109.2(6)	1.536(8)	2.50(1)		
O(12)	109.0(6)	112.0(3)	112.0(3)	1.48(1)		

Ba–O and K–O distances < 3.1 Å

Ba(1)–O(3)	2.553(1)	A–O(1)[b]	2.99(1)
Ba(1)–O(4)	2 × 2.680(7)	A–O(3)[b]	2.65(1)
Ba(1)–O(6)	2 × 2.983(7)	A–O(5)[b]	2 × 3.057(7)
Ba(1)–O(8)	2.99(1)	A–O(9)[b]	2.763(9)
Ba(1)–O(12)	2.56(1)	A–O(10)[b]	2 × 2.809(7)
Ba(2)–O(2)	3.05(1)	K(2)–O(5)	2 × 2.957(8)
Ba(2)–O(3)	2.89(1)	K(2)–O(7)	2.66(1)
Ba(2)–O(5)	2 × 2.797(7)	K(2)–O(8)	2.62(1)
Ba(2)–O(9)	2.804(9)	K(2)–O(9)	3.05(1)
Ba(2)–O(10)	2 × 2.740(7)	K(2)–O(10)	2 × 3.042(8)

[a] Symmetry code: (i) $x, y + 1, z$; (ii) $-x + 0.5, -y + 1, z - 0.5$; (iii) $-x, -y, -z$; (iv) $-x + 0.5, -y, z - 0.5$; (v) $x - 0.5, y, -z - 0.5$; (vi) $x, -y + 0.5, z$.
[b] A = Ba(3) or K(1).

solution is not complete. Because the Ba(2) and Ba(3)/K(1) sites are close enough that they effectively constitute *one* site, there can only be a maximum of three cations per formula unit, so that the most K-rich composition possible, consistent with charge balance, would be "$K_2BaSb_4O_9(PO_4)_2$." Experimentally, this composition is not attained, the observed limit being $K_{0.8}Ba_{1.6}Sb_4O_9(PO_4)_2$. There is an additional repulsion between the K(2) and the combined Ba(2) and Ba(3)/K(1) sites (at 3.0–3.4 Å) that prevents them from being fully occupied by cations. The intermediate members of the solid solution $K_{2x}Ba_{2-x}Sb_4O_9(PO_4)_2$ ($0 < x < 0.4$) are formed by the progressive substitution of Ba with K, as the Ba(2) site is emptied and the Ba(3)/K(1) and K(2) sites are filled.

ACKNOWLEDGMENT

A. M. thanks NSERC Canada for financial support in the form of a postdoctoral fellowship.

REFERENCES

1. Y. Piffard, A. Lachgar, and M. Tournoux, *Mater. Res. Bull.* **20,** 715 (1985).
2. Y. Piffard, A. Lachgar, and M. Tournoux, *Mater. Res. Bull.* **21,** 1231 (1986).
3. Y. Piffard, A. Lachgar, and M. Tournoux, *J. Solid State Chem.* **58,** 253 (1985).
4. Y. Piffard, S. Oyetola, S. Courant, and A. Lachgar, *J. Solid State Chem.* **60,** 209 (1985).
5. A. Lachgar, S. Deniard-Courant, and Y. Piffard, *J. Solid State Chem.* **63,** 409 (1986).
6. R. D. Shannon, *Acta Crystallogr. Sect. A* **32,** 751 (1976).
7. K. Yvon, W. Jeitschko, and E. Parthé, *J. Appl. Crystallogr.* **10,** 73 (1977).
8. C. K. Fair, "MOLEN Structure Determination System." Enraf–Nonius, Delft, 1990.
9. D. T. Cromer and J. T. Waber, *in* "International Tables for X-Ray Crystallography," Vol. IV, Tables 2.2B and 2.3.1. Kynoch Press, Birmingham, England, 1974.
10. P. Coppens, L. Leiserowitz, and D. Rabinovich, *Acta Crystallogr.* **18,** 1035 (1965).
11. A. C. Larson and R. B. Von Dreele, "GSAS, Generalized Structure Analysis System." University of California, 1985.
12. H. M. Rietveld, *J. Appl. Crystallogr.* **2,** 65 (1969).
13. M. Fakhfakh, A. Verbaere, and N. Jouini, *Eur. J. Solid State Inorg. Chem.* **29,** 563 (1992).